

## Chapter 3

### The Proton Synchrotron (PS): At the Core of the CERN Accelerators

Donald Cundy and Simone Gilardoni

#### 3.1 Introduction

##### *The PS accelerator*

After almost 60 years of honourable service, the history of the CERN Proton Synchrotron, PS, is marked by successes and discoveries, intimately linked to the CERN history. Today, the PS is the beating heart of the LHC (Large Hadron Collider) injector complex, the last of the countless successes of this incredible and versatile machine. At the origin of this longstanding success is the foresight of the CERN founding fathers who in the early 1950s took the risk to bet on a new technique in accelerator design called strong focusing [1]. Their “scientific and technological” audacity paved the road of CERN’s future, but also encouraged others to embrace the same spirit of technological enterprise. Conceived as a prototype machine with a life time of only a few years the PS would not only exceed all expectations, but also inspire the design of all the modern circular machines. The PS was and still is an invaluable tool for beam physics studies, and was the cradle of high energy physics for many years, until more powerful machines like the ISR (Chapter 4) started in turn the era of the hadron colliders.

The PS is a synchrotron accelerating particles up to 28 GeV [2–5]. The energy was chosen based on physics considerations, i.e., study particle interactions at the GeV scale, but also economic ones. The initial energy was set well beyond the few GeV scale, up to 30 GeV, but the first machine design was considered too expensive and technologically risky. Fortunately for the future generations of physicists, CERN Council rejected the recommendation of W. Heisenberg to reduce the energy, thus the cost, to 20 GeV, and decided to keep the machine design that reached 25 GeV.

A synchrotron like the PS is a circular ring where particles during acceleration from the lowest to the highest energy are always kept on the same orbit with a constant radius of curvature [Box 2.1]. This is realized by increasing, synchronously with the energy change, the strength of the magnetic elements generating the force that counteracts the centrifugal force acting on the particles. Whereas the synchrotron concept was applied at other places before CERN, like the Cosmotron accelerator in the USA at BNL, the PS was unique with the first ever implementation of the concept of strong-focusing, i.e., the presence in the machine lattice of dedicated beam focusing elements, the quadrupoles. These are elements with properly shaped magnetic fields to control the physical size of the beam, thus limiting the maximum beam dimensions, much as in normal optics lenses would focus the light rays. This can be reached, as in classical light optics, by alternating focusing lenses with defocusing ones, from which the name of alternating gradient lattice was derived. The concept of strong focusing, also called alternating-gradient focusing, was invented in the early 1950s [1], and boldly adopted by CERN in 1952 for the future PS in an incredible gamble: while the cost of the construction could be significantly reduced, because the new focusing principle held the promise of smaller beam and therefore smaller beam elements, this novel idea had never been tested on a real accelerator. The PS was a resounding success, closely followed by its sister synchrotron in the USA, the AGS. All modern accelerators for high energy applications, including the LHC, are based on the strong focusing principle.

The implementation of this technique took a very particular form in the PS [2]: C-shape combined function magnets reaching 1.4 T at 28 GeV were chosen, which combine the functions of bending and focusing of the beam in the same magnetic element, a choice partially motivated by the heritage of the previous accelerators. However, the first-time use of a strong focusing lattice opened also a Pandora's box full of new issues in accelerator physics: having the beam circulating without being lost in the first few turns (the full accelerating cycle takes about 2.4 s, i.e. up to about 1 million turns) requires tight tolerances on magnet geometry and relative magnet alignment of the order of few 100  $\mu\text{m}$  on a machine of 628 m circumference. The required magnetic field quality (i.e. precision) had never been achieved before. For example, the relative spread in deflecting strength of the magnets had to be less than  $5 \times 10^{-4}$ . Despite these challenges, measurements repeated in 2014 confirmed that the magnets, constructed in the first half of the 1950s, were actually better than specified, leaving a sense of awe and admiration for such work realized with the technology available at that time. Another example, the calculation of the beam stability to define the required tolerances, was realized using the first generation of computers available in the UK.

## RF Acceleration

### Box 3.1

The particles in synchrotrons and colliders [Box 2.1] are accelerated by one or more RF cavities. These devices provide an accelerating electric field to increase particle energy per turn or manipulate the bunches (e.g. splitting, merging). Their simplest version is a pill-box in which an oscillating electromagnetic (e-m) field is generated; this provides the longitudinal electric field (Fig. 1). The field does not propagate into the adjacent vacuum chamber; to do so would require a much higher frequency e-m field.

For all cavity types, the e-m field oscillates with a frequency  $f_{rf}$  (wavelength  $\lambda = c/f_{rf}$ ) which is a multiple  $h$  of the revolution frequency  $f_0$  of the particle  $f_{rf} = h \cdot f_0 = h \cdot c \cdot \beta / C$ , where  $\beta = v/c$  and  $C$  the circumference of the ring. Since the RF field is oscillating, the beam cannot be continuous and the particles must come in groups, called bunches. The harmonic number  $h$  defines the maximum number of bunches in the beam. The bunch to bunch distance is  $nC/h$  or in time  $n/f_{rf}$  with  $n = 1, 2, \dots$ . Gaps in the beam can be generated by not filling the positions of a group of bunches, such as when required for injection or extraction. To enable transfer from one circular accelerator  $k$  to the next  $k+1$ ,  $C_{k+1}/C_k$  must be the ratio of two positive integer numbers. For example, LHC/SPS = 27/7, SPS/PS = 11/1. Bunch to bunch distance is preserved at transfer.

If the particle speed is varying during acceleration, which is the case until the particle energy  $E$  exceeds by far its rest energy,  $E_0$ ,  $f_{rf}$  has to vary in synchronism with  $f_0$  and the resonance eigenfrequency  $f_{ef}$  of the cavity needs to be tuned as  $f_{ef}$  has to be very close to  $f_{rf}$ . The difference between  $f_{ef}$  and  $f_{rf}$  is determined by stability criteria [Highlight 3.3]. When  $\beta$  approaches 1, or the cavity is used exclusively at a particular energy, only residual tuning is required to make  $f_{ef}$  close to  $f_{rf}$  to maintain stability. A remotely controlled mechanical device, the tuner, performs this task changing the shape of the cavity slightly. Depending on cavity use, the shape is optimized taking into account RF power requirements, RF power dissipation, peak surface electric fields, and space constraints. This can lead to shapes quite different from the pill-box (Fig. 2). In case powerful acceleration is required, many cavities (cells) are combined in a structure in which either a travelling wave (e.g. 200 MHz RF structure in the SPS) or a standing wave is set up. The RF power is injected via a coupling loop at a point along the structure and is transmitted by em coupling between the cells.

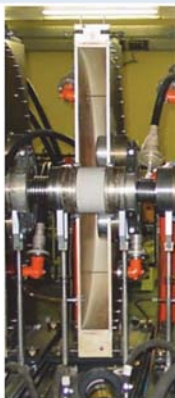


Fig. 1. (Left) Open PS 200 MHz 75 cm diameter ( $\lambda/2$ ) pill-box cavity, with ceramic gap connected to the beam tube [5].

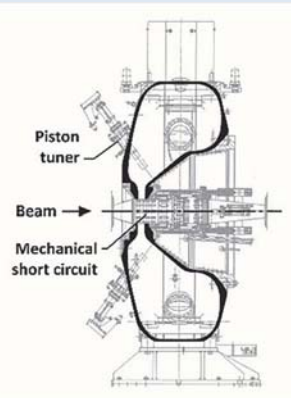


Fig.2. (Right) Cross-section of the PS 80 MHz, 1.8 m diameter cavity, shaped to house the short circuit [5].

The machine took its final shape under the direction of J. Adams during a construction period between 1956 and 1959. The ring is composed of a sequence of 100 main magnets interleaved by 100 straight sections hosting (i) the auxiliary magnets, (ii) the elements for injecting and, later, extracting the beams, (iii) the accelerating radio-frequency (RF) cavities [Box 3.1]. The combined-function magnets shown in Fig. 3.1 are also equipped with a series of windings on their pole-faces to make fine adjustments to the field, a feature substantially enlarging the versatility of the PS.

The machine was assembled on top of a floating floor, mechanically separated from the CERN ground to avoid external disturbances to the machine alignment, e.g. arising from a deformation of the foundation by rain or even earthquake, which would adversely influence the beam orbit.

The first beam was accelerated to 26 GeV in a memorable night of the 24 November 1959, opening both a new era in accelerator physics and in accelerator-based high energy particle physics, an event celebrated in due form on the following day (Fig. 3.2).

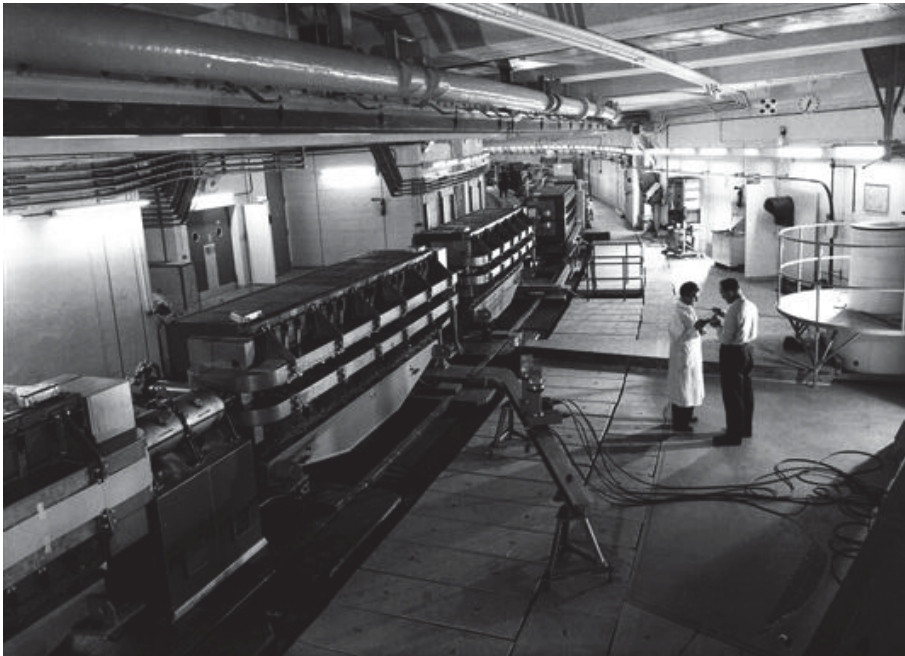


Fig. 3.1. View of the PS ring showing the combined-function magnets.

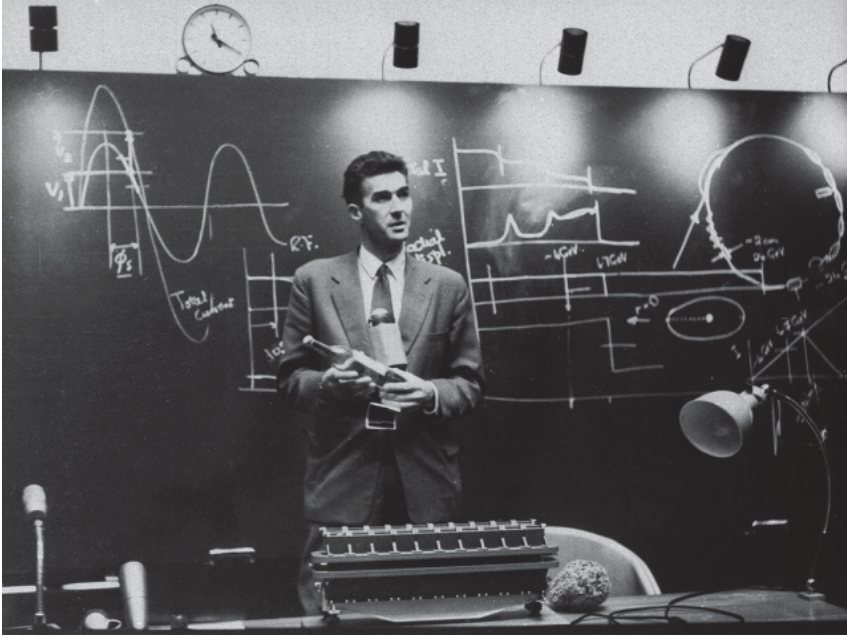


Fig. 3.2. J.B. Adams, the PS project leader, announcing acceleration to 24 GeV in the PS. The Vodka bottle in his hand was a gift from Dubna to be consumed on the occasion of the PS surpassing 10 GeV, the energy of the Dubna Synchro-Phasotron.

Once the basic features of the accelerator were understood, the PS and its injection systems underwent a long series of gradual improvements of performance, reliability and versatility leading to new applications. One indication is the gradual rise of the PS intensity over the years spanning from the design value of  $\sim 10^{10}$  protons per pulse to more than  $3 \times 10^{13}$  achieved for the latest neutrino experiment (Fig. 3.3).

High energy physics research at the PS started first with internal targets and later in 1960 with dedicated beam lines receiving protons by fast or slow extraction. These novel beam extraction techniques were developed with the aim to suppress the originally installed internal targets, source of substantial beam loss, producing a high radiation dose to the machine elements, in particular to the main magnets, and a serious risk to the machine lifetime. Extraction of the beam reduced the internal losses. The external targets allowed higher impacting intensities and could be placed at positions optimal for the experiments [Highlight 3.2].

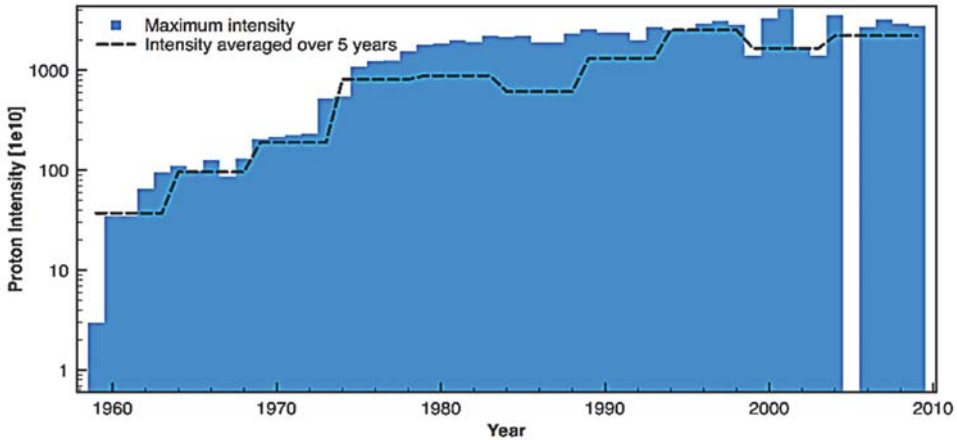


Fig. 3.3. Protons per pulse as a function of time. The PS was stopped for consolidation in 2005.

Special attention has always been paid to the PS injectors [6]. The first injector was a linear accelerator constructed by industry (Linac1) providing 50 MeV protons. In 1965 an improvement programme of the PS was launched together with the approval of the ISR (Chapter 4). The PS beam intensity was increased by inserting a small synchrotron between Linac1 and the PS, the PS Booster (PSB) [Highlight 3.4]. This novel type of accelerator of very compact design combines four synchrotrons in one ring with common bending and focusing magnets. Its potential turned out to be enormous, probably even a surprise to its designers, brought to life by a tenacious development since its first operation in 1972. Not only helped it to increase the intensity in the PS by combining the output of the four rings, but the 16 times higher beam energy compared to Linac1 made the beam stiffer moving the intensity limit at PS injection beyond the intensity provided by the PSB. This intensity limit was later further raised by successive steps in the PSB's output energy from the original kinetic energy of 0.8 GeV to 1.4 GeV. This was indispensable to catch up with the steadily increasing PSB output intensity, raised by a factor eight since 1972. However, the PS did not remain the only client of PSB: ISOLDE [Highlight 3.8] had been moved from the SC to the PSB in order to benefit from the higher proton intensities at the PSB, an elegant solution, because ISOLDE uses only those PSB pulses which are not injected into the PS. A new CERN-designed 50 MeV linac (Linac2) was added in 1978 to improve not only the performance but also the availability of the PSB. Linac1 had already earlier shown its versatility by accelerating deuterons and alpha particles for the ISR but when no longer needed for proton operation it was modified to provide oxygen and sulphur beams to the PS for fixed-target physics

at the SPS. However, it was unsuitable for the acceleration of heavier ions so one resolved to replace Linac1 with Linac3 of modern design providing nowadays mainly lead ions to the LHC, but also indium and argon ions for the SPS.

The venerable PS still provides a variety of hadron beams including antiprotons (Chapter 6). It also supplied electrons and positrons of 3.5 GeV to the SPS for LEP (see Chapters 5 and 7). To this end, it was equipped with the appropriate acceleration systems, injection/extraction elements and a 600 MeV electron-positron linac as injector feeding a small accumulation ring preceding injection into the PS. In view of improving the LHC injector performances, Linac2 will be replaced by a new linac accelerating negative hydrogen ions to 160 MeV (Linac 4). In order to cope with the concurrent intensity increase, the PSB output energy will be raised in another step to 2 GeV, 2.5 times the design energy, another proof of the PSB's amazing inherent potential.

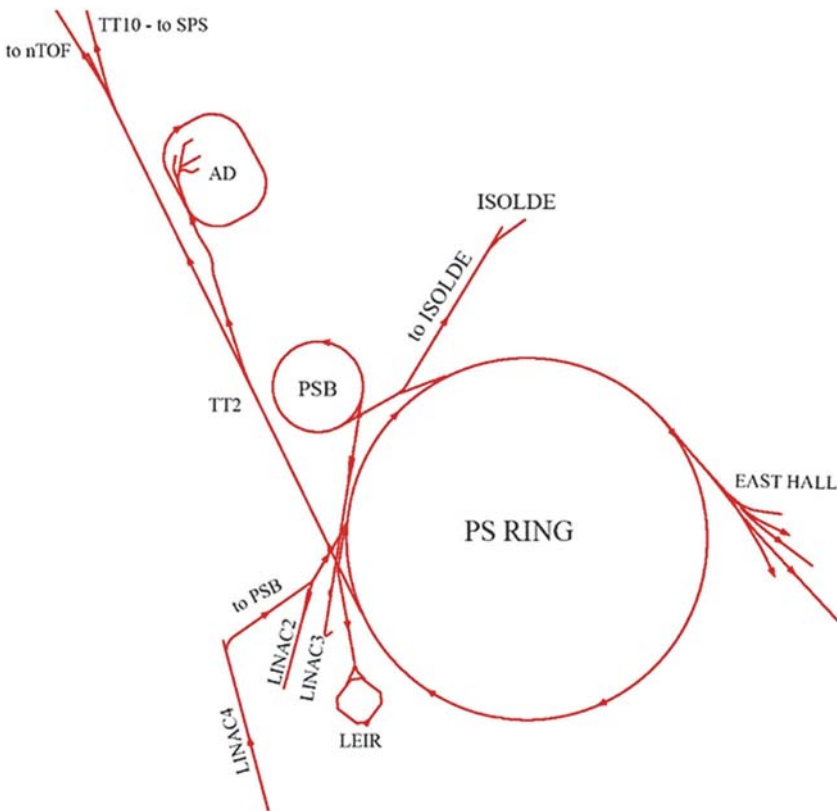


Fig. 3.4. Layout of the injectors and beam lines to the experiments.

The PS is still at the core of producing proton and ion beams as shown in Fig. 3.4 for fixed-target physics at the PS, the Antiproton Decelerator (AD), the SPS, and for the LHC. The LHC collider operates with two different bunch spacing, either 50 ns or 25 ns, the latter being the design configuration. Subtle manipulation of the beam by RF [Highlight 3.3] determines this bunch spacing in the PS and the downstream accelerators. Continuing a 60-year long tradition of attentive care, its infrastructure is maintained to keep up with the ever-increasing demand. A shining example is the novel solid-state main power converter with capacitive energy storage replacing the more than 30-years old rotating machine, which used a flywheel or energy storage to smooth the load to the mains [Highlight 3.5]. The new technology proved to be so successful that it inspired colleagues of the sister synchrotron AGS in the USA to consider also replacing their rotating machine.

A most flexible design, high-quality components and vigorous consolidation programmes for the accelerator and its infrastructure are the basis for the surprising durability of this synchrotron which proved, every time it was called upon a new task, its adaptability, versatility and reliability. This venerable machine stayed and will stay for many years at the heart of the CERN accelerator complex, a fine example of the continuous (re)use of CERN infrastructure.

### ***The PS experimental programme***

When the CERN PS was ready for physics in 1960, particle physics had entered a Golden Age of “particle discovery”. Strange particles, collected painstakingly using cosmic rays, were now being produced copiously at the proton synchrotrons. The electron-neutrino  $\nu_e$  had been detected. The antiproton and the antineutron had been discovered. Parity Violation (PV) in Weak Interactions (WI) was proven in 1956. However, theoretical guidance was still weak or absent: the quark hypothesis was made in 1964, followed by the electroweak theory in the late 1960s, the SM by the end of the sixties, and the theory of strong interactions (QCD) in 1973 [Boxes 4.2, 6.4]. The physics landscape and major PS results are reviewed in [7].

The bubble chamber (BC), invented in 1953, had become, with gradual improvements, the detector *par excellence* [Box 3.3 and Highlight 5.7]. The hydrogen BC, providing a proton target, lent itself to the detailed study of particle production, whilst the heavy liquid BCs proved very useful in the study of weak decays of the new particles. However, these BCs have a serious drawback: the repetition rate, i.e. their data taking rate is very low and they lack the capability of selecting specific events.



**Particles interacting with matter****Box 3.2**

To be detected, a particle must transfer some of its energy to the detector material [Box 6.3]. The nature of the interaction — electromagnetic (e-m), strong, weak — depends on the particle charge and quantum numbers. A *charged particle* excites (*ionizes*) the medium through which it passes: this can produce a measurable signal, the basis for most detectors. Tracking detectors record *ionization* produced along the trajectory of charged particles [Highlight 4.8]. The ionization energy loss  $dE/dx$  depends on the particle velocity  $v$  and may provide a measure of  $v$ ; if the particle momentum  $p$  is known, its mass can be determined [Box 5.2]. Some media exhibit the property of *scintillation*: a charged particle traversing matter leaves a trail of excited molecules which release part of this energy as photons. Although only a few percent of the total energy loss, it is sufficient to detect a particle. Besides colliding with atomic electrons, a particle, shaken by the e-m fields in the material, emits *radiation* at a rate roughly proportional to  $E/m^2$ . This process is characterized by the *radiation length*  $X_0$  of the medium, over which an  $e^\pm$  has lost all but  $1/e$  of its energy, and a  $\gamma$ -photon has a  $2/3$  probability to convert into a  $e^\pm$  pair. Typical values of  $X_0$  are 1.8 cm (Fe) and 300 m (air 1 atm). Above a critical energy  $E_c$ , radiation effects (bremsstrahlung for  $e^\pm$ , pair conversion for  $\gamma$ 's) dominate over ionization energy loss. For  $e^\pm$ ,  $E_c$  is a few tens of MeV for most materials; heavier muons have a critical energy of several hundred GeV. Two metres of iron absorb most particles except muons, so muons are usually measured behind hadron calorimeters [Highlight 7.10]. *Neutral particles* are not sensitive to e-m effects. If unstable, they can be detected by tracking charged decay products [Highlight 8.6]; if stable or long-lived (e.g. neutrons), detection is ensured via strong interactions in devices such as calorimeters [Highlight 4.10]. *Hadrons* — baryons (e.g. the proton) and mesons (e.g. the pion) — interact strongly, producing a *hadron shower*, a process characterized by the *nuclear interaction length*  $\lambda$  (for iron,  $\lambda = 17$  cm), the mean path length over which energetic hadrons have a  $\sim 2/3$  probability to interact inelastically. About  $10 \lambda$  absorbs a 100 GeV hadron. Among *leptons*, neutrinos ( $\nu$ ), neutral, stable and weakly interacting, are the most difficult to detect: a 10 GeV  $\nu$  has only a  $10^{-7}$  probability to interact when crossing the Earth! To observe  $\nu$  interactions requires massive detectors and large  $\nu$  flux. A  $\nu$  escaping from an interaction can be inferred from its “*missing momentum*” vector by measuring all detectable particles. In e-m collisions a charged particle is deflected stochastically: the *mean deviation angle* is proportional to  $vt/p$ , where  $t$  is the thickness of the material in units of  $X_0$ . This impacts on the accuracy of tracking and explains the need for detectors with low total  $t$ . Other e-m energy loss mechanisms are (i) the *Cherenkov effect*: a charged particle traversing matter produces a trail of polarized molecules along its path, which depolarize and emit radiation. If the velocity  $v > c/n$ ,  $n$  being the refractive index of the medium, there is a direction along which the radiation adds coherently, giving “*Cherenkov light*” (analogous to a sonic boom), emitted at the *Cherenkov angle*  $\theta_c$ , where  $\cos \theta_c = c/nv$  [Highlights 7.8, 8.10]; and (ii) *Transition Radiation (TR)*, which occurs when a charged particle passes between media of different permittivity. It is used to identify ultra-relativistic electrons [Highlight 4.9].

This motivated the development of “electronic”, triggerable detectors, such as spark chambers, scintillation counters and threshold Cherenkov detectors for particle identification [Boxes 3.2 and 6.3]. It culminated in the invention of the “Multi-wire proportional chamber (MWPC) in 1968 [Highlight 4.8]. Counter and emulsion experiments studied secondary particle production ( $\pi$ , K, antiprotons) from various targets located in the PS beam. These studies were to have strong impact on the design of separated beams that were soon to be built.

While the PS machine was built in a remarkably short time, CERN’s start of its physics programme was rather more shaky. There were, it should be noted, not so many physicists participating in the research programme at CERN at that time, as the larger member states were still pursuing their national projects. Fortunately for the development of particle physics, there was still at that time strong political and financial support given to both nuclear and particle physics.

In 1960 one of the big puzzles in particle physics was the muon, which decays into an electron and two neutrinos. What prevents the muon from decaying into an electron and a gamma ray? An elegant hypothesis gives the electron and muon a hidden property (“quantum number”), which stipulates the existence of two neutrinos *species*, one related only to the muon,  $\nu_\mu$ , and another one associated to the electron,  $\nu_e$ . Neutrino scattering it was argued, could test this hypothesis:  $\nu_\mu + n \rightarrow p + \mu^-$  and  $\nu_e + n \rightarrow p + e^-$ .

A source of  $\nu_\mu$  is the pion, decaying essentially into a muon and a neutrino. Early in 1960 it had been argued that pions, produced at accelerators like the PS, would give enough  $\nu_\mu$ ’s to perform a conclusive experiment. CERN jumped on this idea with great enthusiasm, because of its conceptual simplicity and physics importance. In the South Hall pions were produced on an internal target in the PS, which subsequently decayed in a 20 m space, followed by some 20 m of iron and concrete shielding. The main detectors were the CERN and the Ecole Polytechnique BP3 heavy liquid bubble chambers containing a total of about a ton of  $\text{CF}_3\text{Br}$  Freon. The expected rate was around one event per day. However, a last minute beam survey showed that the pion flux would be an order of magnitude below design and the experiment was stopped. CERN lost its chance for a big discovery, the muon neutrino. Only one year later, in 1961, the two-neutrino hypothesis was confirmed in a Brookhaven experiment using the same method and a spark chamber detector!

Despite this sobering setback, neutrino physics would develop into a very important field of research at CERN and elsewhere. The radioactive decay of particles due to the weak interaction occurs at relatively low energies. In contrast, neutrino scattering would probe the weak interactions at much higher energies and

**Imaging detectors****Box 3.3**

These provide an image of particle tracks, usually recorded photographically.

*Nuclear emulsion (NE)* is a photographic plate with a thick layer of emulsion of uniform grain size. Compact and dense, it has the best spatial resolution of all, at the  $\mu\text{m}$  level. A crossing charged particle sensitizes the grains. After development, tracks are visible and measured with a microscope. NEs have undergone a renaissance, coupled to fast precise electronic detectors, which point to the region of interest.

The *cloud chamber (CC)* is a sealed environment containing a supersaturated vapour of water or alcohol. Charged particles ionize the vapour and the ions act as nuclei for condensation. Mist forms around the ions to produce a visible track. In a *pulsed CC or Wilson chamber* (C.T.R. Wilson, Nobel 1927), a diaphragm expands the volume which cools and initiates condensation. Positrons and muons were discovered in cosmic rays using CCs. A *diffusion CC* is continuously sensitive, but needs cooling.

The *bubble chamber (BC)*, (A. Glaser, Nobel 1960), is similar in principle to a CC: a cylinder is filled with a liquid heated to just below its boiling point. A piston suddenly expands its volume, lowering the pressure and driving the liquid into a superheated metastable phase. Microscopic bubbles form along the ionization track. Their size grows as the BC expands, getting large enough to be photographed. Adding a magnetic field gives the momentum. More than 100 BCs were built [1], from very small to very large. The largest contained up to  $40\text{ m}^3$  of liquid hydrogen or heavier liquid (e.g. freon) and were used to record millions of images. Momentum resolution depends on the BC size, the magnetic field and the bubble size, ranging from typically  $200\ \mu\text{m}$  to  $700\ \mu\text{m}$  in diameter in BEBC [Highlight 5.7]. To study charm requires bubbles of  $30\ \mu\text{m}$ . Photographing such details limits the depth of field of the camera and the observable volume. This led to develop small rapid cycling BCs, e.g. LEBC [1].

The BCs were facilities, operated by large laboratories and used by many groups, leading to international collaborations, sharing the scanning and measuring of BC photos. Ever more elaborate analysis methods were developed, implying semi-automatic data recording and the use of powerful computers. These pictures, providing an intuitive view of physics events, helped to popularize the field. But restricted to fixed target physics, unable to be triggered and of low pulse rate, BCs could not give access to rare events and were progressively abandoned.

The *spark chamber (SC)* [2] uses the breakdown induced by a strong electric field locally around the particle trajectory. These “sparks” can be photographed or recorded electronically. A sequence of SCs provide a BC-like detailed view of the particle track. The two-neutrino US experiment (Chapter 3.1) used the first large SC set up. The largest one at CERN was the Omega spectrometer [Highlight 3.7]. *Streamer chambers* with shorter high-voltage pulses and image enhancement also used gaseous breakdown providing bubble-chamber type views of particle collisions.

From 0.01 Hz for CC, the pulse rate went to 0.3 Hz in BEBC and up to 20 Hz in SC. Discoveries made with these devices were essential in establishing the SM [Box 6.4].

[1] G.G. Harigel *et al.*, (ed.), Proc. Conf. on Bubble Chambers, *Nucl. Phys. B, Suppl.* **36** (1994).

[2] R.P. Schutt, (ed.), *Bubble and Spark Chambers* (Academic Press, New York 1967).

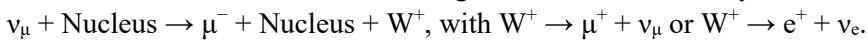
would also allow to investigate the interior of the nucleon. Neutrino scattering would shed light on the fundamental nature of this mysterious weak interaction. At high energies, it was understood, a new mechanism has to be invoked, a particle, technically called “Intermediate boson” (IB), had to exist to transmit or “mediate” this interaction. This idea was worked out in the 1960s, although its mass was a mystery, justifying early searches at quite low masses. The chase for the IB would become one of the grand successes of CERN (Chapter 6).

There were other questions: is the “lepton property”, the so-called lepton number conserved? Could a neutrino interact with a nucleon without changing into a charged lepton, i.e. besides the known “Charged Currents” (CC) of muon and beta decay, did “Neutral Currents” (NC) exist?

### Towards neutral currents

CERN had learned its lesson: To run a viable neutrino research programme neutrino beams of adequate intensity were required. Step 1 was to maximize the pion flux, achieved by extracting the PS proton beam towards an external target in the direction of the experiments. Step 2 was a real breakthrough: the ingenious invention by S. van der Meer (Nobel Prize 1984) of a pulsed magnetic horn, focusing the pions, produced with different momenta and angles at the target, towards the detector and hence maximizing the neutrino flux [Highlight 3.6].

The beam was ready in 1963; the detectors were the CERN Heavy Liquid BC (HLBC) and a 15 ton spark chamber (SC) setup. The BC team would study the neutrino reactions in detail and measure cross-sections of specific processes. The SC group was primarily searching for the possible production of the IB ( $W^+$  or  $W^-$ ) with a mass below 2 GeV in the strong electric field of a heavy nucleus:



At the September 1963 Siena Conference, the two experimental teams presented their preliminary results, the BC with a couple of hundred events and the SC setup with many thousands. The former presented results on the cross-section measurements of the elastic process  $\nu_\mu + n \rightarrow \mu^- + p$ , the quasi-elastic process  $\nu_\mu + p \rightarrow \mu^- + \Delta^{++} \rightarrow \mu^- + p + \pi^+$ , on the energy dependence of the total cross-section and many other topics. The latter reported several di-muon candidates but could not say if they were W decays. The future was decided in a local trattoria: a very large heavy liquid BC with its splendid detail about the interactions was the way to move forward. It had to have a large target mass for a reasonable interaction rate and several interactions in length to distinguish pions from muons.

The proposal made to the French CEA was accepted and funded in 1964. In 1965 CERN agreed to host the heavy-liquid BC and to build a new neutrino beam. The BC was a cylinder 4.8 m long and 1.9 m in diameter with a volume of 12 m<sup>3</sup>,

bright field illumination, six cameras and a magnetic field of 2 T. It would be known as Gargamelle (Fig. 3.5, left). The intellectual father and project leader was A. Lagarrigue (Fig. 3.5, right).

While waiting for Gargamelle, the CERN HLBC, which had been doubled in size, was filled with propane and exposed to the new beam. About this time a US group studying neutrino electron scattering at a nuclear reactor had reported a single electron signal three orders of magnitude greater than theoretically expected. A careful search for single electrons in the HLBC propane photos did not find any event, placing new upper limits on the “neutral current” processes  $\nu_\mu + p \rightarrow \nu_\mu + p$  and  $\nu_\mu + p \rightarrow \nu_\mu + n + \pi^+$ . The reported claim was eventually withdrawn.

When data taking started in 1971 with Gargamelle, priority was given to measure the CC total cross-section and to probe the nucleon structure. The reason was that electron scattering experiments at SLAC had shown the nucleon to contain point-like constituents. Combining neutrino data with the electron data would allow to measure the charge and net number of these point-like particles.



Fig. 3.5. Left: inside Gargamelle. Right: A. Lagarrigue, the driving spirit of Gargamelle.

However, early 1972, priorities were reversed. The Electroweak (EW) theory, unifying the weak and electromagnetic interactions, had been completed [8]. Crucially, it predicted the existence of a heavy *neutral* Intermediate Boson. Neutral Current (NC) events would therefore occur, revealed by a single recoil electron or by hadron production as in a CC event, but without a muon (Fig. 3.6). All efforts were devoted to scanning Gargamelle photos for single electrons and searching NC candidates with hadronic energy greater than 1 GeV. Studies on possible background events convinced the collaboration that neutrons coming from neutrino interactions in material around the detector were the only significant

background, which however could be evaluated and controlled. In addition, one NC candidate event with a single electron had been found in the antineutrino exposure where this background was negligible.

A competing US experiment produced contradictory results and some confusion. However, sure about their results, the Gargamelle collaboration announced and published their evidence for the existence of neutral currents in July 1973 with the measured ratio  $NC/CC = 0.21 \pm 0.03$  for neutrinos and  $NC/CC = 0.45 \pm 0.09$  for antineutrinos [9]. This result was a turning point in the history of particle physics, leaving little doubt about the validity of the EW SM, allowing to predict the weak bosons masses with small errors and opening the modern era of precision tests of the SM. The premature death of A. Lagarrigue probably deprived the neutral current discovery of a Nobel Prize.

Other results followed. The total neutrino-nucleon cross-section was found to rise linearly with energy, consistent with point like objects in the nucleon, confirming with the weak probe the earlier SLAC observation with the electromagnetic probe. Combining both results showed that these constituents have indeed fractional charges.

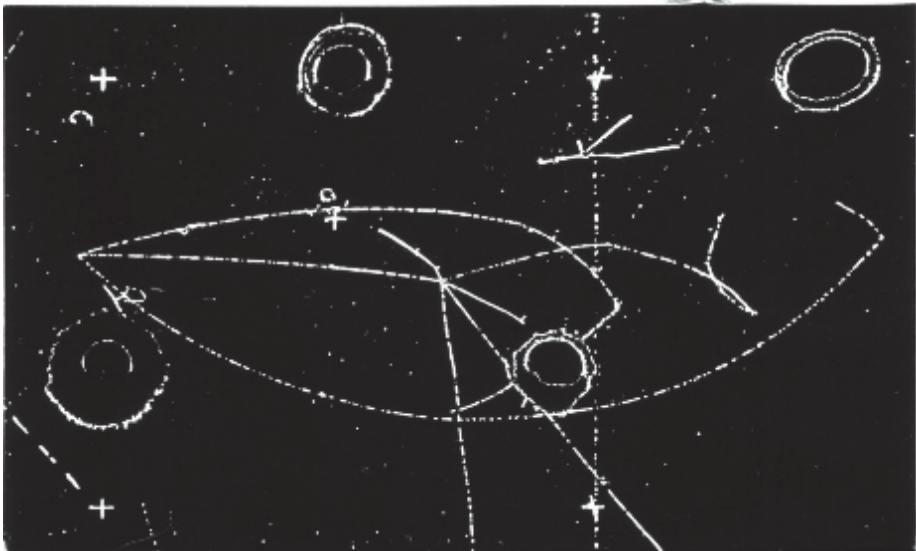


Fig. 3.6. A neutral current event in Gargamelle. The neutrino beam enters from the left. All three tracks from the collision vertex either undergo very large angle scattering or interaction, proving that no muon is produced.

Interestingly, a neutrino beam was again derived from the PS in the early 1980s, aiming at the West Area neutrino detectors in search of neutrino “oscillations”, i.e. their “morphing” along their way, from a muon-neutrino to an electron- or tau-neutrino. As realized later, neutrino oscillations indeed exist, but with periodicities not experimentally accessible at CERN. Nevertheless, the experiments, e.g. PS191, were visionary and pioneering in their concept.

After its difficult start the PS neutrino programme had turned out to be quite remarkable!

### **Other programmes**

In 1960 CERN reorganized their experimental activities in response to the changing nature of the experiments and their techniques. With the aim of strengthening the research programme the experiments using counter techniques and those with bubbles chambers were supported in separate dedicated Divisions.

### ***Hydrogen bubble chambers at the PS***

During the PS time BCs increased in size from 30 cm to 2 m size, and were exposed to an increasing variety of hadron beams.

Coping with the enormous number of BC photos led to R&D programmes for the machine inspection (scanning) of the BC pictures. Semi-automated or fully automated measurement equipment on digitizing tables were developed; computer programs were developed to analyse and interpret the events [10].

The list of new particles and resonances became ever longer. Cross-sections were measured with great precision and particle production mechanisms studied in detail. The CERN PS experiments made significant contributions. Various theoretical models came and went until it was eventually realized that this zoo of particles could be best described by the model of fractionally charged quarks by M. Gell-Mann and G. Zweig, then a visitor in the CERN Theory Division [11].

One of the most important spinoffs of the BC program was sociological: it attracted many European university teams in particle physics and contributed to fostering a culture of fruitful collaboration among different nationalities: The building of this aspect of the “CERN model” got on its way.

### ***Experimentation with electronic detectors***

Research, increasingly concentrating on phenomena occurring with very small cross sections and using a variety of particle beams, motivated a rapid growth and diversification of the electronic detectors. Scintillation counters, Cherenkov detectors and spark chamber became the “workhorses” of ever more sophisticated experiments based on these electronic techniques. The 1968 invention of the Multiwire Proportional Chamber (MWPC) by G. Charpak, Nobel Prize 1992, truly initiated this electronic revolution.

Initially, the spark chambers events were recorded photographically, soon to be replaced by acoustic, magnetic core and magnetostrictive readout. In 1964 a meeting was held at CERN on “Film-less Spark Chamber Techniques and Associated Computer Use” [12]. This led to the wire spark chamber, invented at CERN, in which the plates were replaced by wires. The “sparks” produced electrical pulses in the wires, which were directly logged into a computer. This was the start of using computers for monitoring and data recording of the experiments.

One experiment, using a combination of dipole and quadrupole magnets and an electrostatic separator, followed by a very sophisticated Time-of-Flight system discovered the production of anti-deuterons in proton–beryllium collisions, preceding a similar observation at BNL by a few weeks. The existence of the bound state of antinucleons was essential for the proof of the existence of antimatter, as Dirac liked to emphasize. It also lent credence to the concept of a fundamental symmetry, the so-called Charge–Parity–Time Reversal (CPT) symmetry [Box 2.2], fundamental to quantum field theories, such as the SM.

The rise of electronic detectors motivated a bold decision to develop an “electronic bubble chamber”, a large 1.8 T magnetic field volume, instrumented with spark chambers, capable of selecting (triggering on) specific reactions. The device was known as OMEGA [Highlight 3.7]. At the PS it was used from 1971–76 to study meson spectrometry and rare modes of hadronic reactions, and subsequently in a productive program at the SPS, with spark chambers being replaced by MWPCs.

CP violation [Box 3.4] was discovered at Brookhaven in 1964 and the result quickly confirmed at CERN, eliminating some theoretical models and correcting some erroneous claims made elsewhere.

Experiments using the interference between the charged two-pion decay of  $K_S$  and  $K_L$  performed precise measurements of the  $K_S$ – $K_L$  mass difference, the CP violation amplitude and phase [Highlights 5.5 and 5.6]. In 1969 one of these experiments began to use the first very large MWPC chambers. In 1972 a setup using wire chambers and a lead glass array proved that the ratio of the CP violating amplitudes of the two-pion charged and neutral decay of  $K_L$  was equal to unity to a 6% level. It would take another 20 years to know that they differ from unity at the per mille level (Chapter 5, SPS).



**Kaon mixing and CP violation**

**Box 3.4**

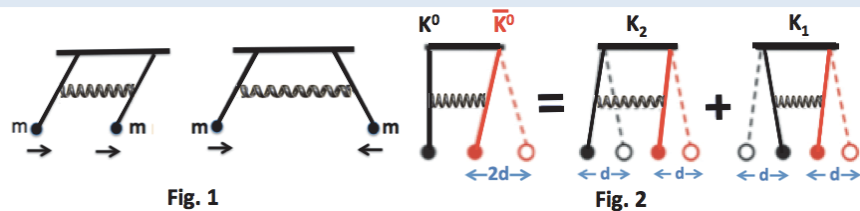
The  $K^0$  shows a puzzling behaviour: It decays via the weak interaction in  $\sim 10^{-10}$  s into two  $\pi^\pm$  or two  $\pi^0$ , called  $K_1$ , and 600 times slower into three pions ( $\pi^+$ ,  $\pi^-$ ,  $\pi^0$  or  $3 \pi^0$ ), called  $K_2$ ! The explanation is that the  $K^0$  can change into an anti- $K^0$  ( $\bar{K}^0$ ), and vice versa, by virtual decay and recombination. The decay modes observed are the symmetric ( $K_2$ ) and antisymmetric ( $K_1$ ) quantum state combinations of  $K^0$  and  $\bar{K}^0$ . This seems complicated, but is simple and has a classical analogue of two coupled pendula, Fig. 1.

For two identical pendula, coupled by a spring (Fig. 1), only two modes of oscillation can exist: parallel (P) and antiparallel (AP). One can ascribe a *symmetry* to the pendula under which the AP (P) mode is considered an even (odd) state. The spring is at work in the AP mode only, and hence it will have a slightly higher frequency than the P mode. If the spring is not perfect, it costs energy and the AP mode will decay away quicker than the P mode. Setting in motion e.g. the right pendulum (left of Fig. 2) the spring will transfer energy between the two pendula, such that the left one starts and the right one comes to rest, and vice versa. This is due to the interference (beating) between the two modes. The antiparallel mode is damped and will decay away first.

In our particle picture, assume the *motion* of the left (right) pendulum to represent a  $K^0$  ( $\bar{K}^0$ ), Fig. 2. The right pendulum describes an initial *pure*  $\bar{K}^0$  state. The spring provides the interaction which changes the  $K^0$  and  $\bar{K}^0$  into each other. Fig. 2, right part, shows that the  $K^0$ - $\bar{K}^0$  system can be considered as the superposition of the P (odd) mode, representing a  $K_2$ , and the AP (even) mode, representing a  $K_1$ . The spring is not perfect and the antiparallel mode  $K_1$  is damped first, leaving the long lived  $K_2$ . The two different  $K_1$  and  $K_2$  decay rates are reproduced. The decays were considered to be invariant under CP, i.e. CP to be a good or conserved symmetry in the weak interactions [Box 2.2]. The symmetry ascribed above to the pendula is the mechanical equivalent to CP symmetry seen in the kaon system.

If CP were a perfect symmetry, then the CP odd  $K_2$  should not decay into a CP even  $2\pi$  state: but in 1964 one found that it did at the  $10^{-3}$  level, showing that CP is violated in  $K^0$  mixing:  $K^0$  and  $\bar{K}^0$  do not change into each other at the same rate. This kind of CP violation is demonstrated with the coupled pendula by connecting the spring at different positions on the  $K^0$  and  $\bar{K}^0$  arms. Then the energy transfer between the two pendula is not equal: the long-lived mode contains a small part of  $K_1$ , is no longer a pure CP state, and is called  $K_L$ . The short-lived mode contains some  $K_2$  and is called  $K_S$ .

Due to mixing the amount of CP violation seen in the decay mode into two  $\pi^\pm$  should be the same as for the decay into two  $\pi^0$ . This is only true down to the  $10^{-6}$  level, where so-called *Direct CP violation* is also observed [Highlight 5.5]. Related effects are observed in the decay of B-mesons, particles containing a beauty quark [Highlight 8.6].



The PS measurement of the anomalous magnetic moment of the muon,  $g - 2$ , [Highlight 2.4], successfully continued the tradition started at the SC. With a 5 m diameter storage ring experiment (1967–1970) an accuracy of 3 parts in  $10^4$  was reached, to be superseded with a new storage ring of 7 m (1972–76), which reached an accuracy of 1 part in  $10^5$ . Today, higher order QED calculations, including weak and hadronic corrections, predict  $g - 2$  with an accuracy of 1 part in  $10^6$  and ongoing experiments elsewhere are being pushed to achieve an even higher accuracy. An observed slight discrepancy between the theoretical and experimental value, if it persists, would be a “smoking gun” for new physics.

### Other facilities

Besides supplying protons for the SPS and the LHC, the PS also feeds some other very important facilities, ISOLDE, n\_TOF and CLOUD.

The PS Booster’s high intensity 1.4 GeV proton beam is directed onto special thick targets of the ISOLDE facility [Highlight 3.8], from which beams of radioactive isotopes are obtained.

For the n\_TOF facility 20 GeV/c proton pulses, 6 ns long, are directed onto a lead target producing spallation neutrons in a wide energy range [Highlight 3.9]. These neutrons travel  $\sim 20$  or 200 m to the experimental areas depending on the flux required. The energy of the neutrons is measured by time-of-flight. Research ranges from stellar nuclear synthesis to studies of nuclear reactor fuel cycles.

An experiment involving atmospheric, cosmic ray and particle physicists, and chemists, the Cosmics Leaving Outdoor Droplets (CLOUD) project, is studying the very complex processes of cloud formation under the influence of cosmic rays. The PS supplies the particle beams that simulate cosmic ray flux [Highlight 10.7].

## 3.2 Extraction: Getting the Beam to Leave the Accelerator

Massimo Giovannozzi and Charles Steinbach

Originally, the PS had used only internal targets. However, high radiation damage, due to absorption of secondary particles in the accelerator components, and low efficiency motivated the development of beam extraction and external targets. Fast extraction provides a beam with a length of one turn or less in one shot for users requiring high intensity in a short pulse, e.g. for experiments with bubble chambers; slow extraction skims off the circulating beam over many turns and is the choice for counter experiments preferring a long spill length and low instantaneous intensity to match their limited time resolution [13]. In 1963, the PS was the first synchrotron with a fast extraction system in operation and equipped with a successfully tested slow extraction system, initiating a leading position of CERN in the development and improvement of these key techniques.